Title

Polymer-Induced Liquid Precursor (PILP) remineralization of artificial and natural dentin carious lesions evaluated by nanoindentation and microcomputed tomography

Authors

Babaie, Elham

Bacino, Margôt

White, Joel

et al.

Publication Date

2021-06-01

DOI

10.1016/j.jdent.2021.103659

Peer reviewed

HHS Public Access

Author manuscript

J Dent. Author manuscript; available in PMC 2022 August 06.

Published in final edited form as:

J Dent. 2021 June ; 109: 103659. doi:10.1016/j.jdent.2021.103659.

PILP remineralization of artificial and natural dentin carious lesions evaluated by nanoindentation and microcomputed tomography

Elham Babaie[a], **Margôt Bacino**[a], **Joel White**[a], **Hamid Nurrohman**[a,b], **Grayson Marshall**[a], **Kuniko Saeki**[a], **Stefan Habelitz**[a,ł]

[a]Department of Preventative and Restorative Dental Sciences, UCSF School of Dentistry, San Francisco, CA, USA

[b]Missouri School of Dentistry and Oral Health, A.T. Still University, Kirksville, MO, USA

Abstract

Objectives: The study evaluates the efficacy to remineralize artificial and natural dentin lesions through restorative dental procedures that include the Polymer-Induced Liquid Precursor (PILP) method comprising polyaspartic acid (pAsp).

Methods: Novel ionomeric cement compositions based on bioglass 45S5 and pAsp mixtures, as well as conditioning solutions (conditioner) containing 5 mg/ml pAsp, were developed and tested on demineralized dentin blocks (3-4 mm thick) on shallow and deep lesions with the thickness of 150 μm ± 50 and 700 μm ± 50, respectively. In the first treatment group, 20 μl of conditioner was applied to demineralized shallow (n=3) and deep (n=3) lesion specimens for 20 s before restoration with glass ionomer cement (RMGIC). For the PILP cement treatment group, cement was applied onto the wet surface of the demineralized specimen for both shallow (n=3) and deep (n=3) artificial lesions after the application of the conditioner and before the final restoration. Sample groups were compared to RMGIC restoration, for both shallow and deep lesions (n=3 each) and treatments in PILP-solution (n=3 for deep lesions) without restoration for 4 weeks. All of the restored specimens were immersed in simulated body fluid (SBF) solution for 2 weeks and 4 weeks for shallow and deep lesions respectively to allow for remineralization. The

[ł]Corresponding author: stefan.habelitz@ucsf.edu (S. Habelitz).

Credit of Authors Statement

E. Babaie did experimental work, performed data analyisis, wrote and revised the manuscript.
M. Bacino did experimental work, performed data analysis and revised the manuscript.
J. White did experimental work, restored the tooth specimens and revised the manuscript.
H. Nurrohman did experimental work, designed the cement formulations and revised the manuscript.
G.W. Marshall did conceptual design and wrote and revised the manuscript.
K. Saeki did conceptual design and revised the manuscript.
S. Habelitz directed the study, did experimental work, wrote and revised the manuscript.

Declaration of interests

The authors declare that they have no known competing financial interests or personal relationships that could have appeared to influence the work reported in this paper.

artificial lesion specimens were evaluated for changes in the nanomechanical profile (E-modulus and hardness) using nanoindentation. Shallow lesions were analyzed by SEM under vacuum for changes in morphology caused by PILP treatments. Also, a pilot study on human third molars with moderate lesions in dentin (n=3) was initiated to test the efficacy of treatments in natural lesions based on mineral densities using microcomputed tomography (μCT) at 0, 1, and 3 months.

Results: This study showed that functional remineralization of artificial lesions using PILP-releasing restoratives occurred, indicated by an increase of the elastic modulus in shallow lesions and in the middle zone of deep artificial lesions. The mechanical improvement was significant when compared to RMGIC restoration without pAsp ($P<0.05$). Nonetheless, recovery across artificial lesions was most significant when specimens were immersed into PILP-solution with restorative ($P<0.01$). Furthermore, natural lesions increased in mineral volume content to a higher degree when the restorative treatment included the PILP-method ($P<0.05$). However, none of the natural lesions recovered to full mineral degree regardless of the treatments.

Clinical significance/Conclusion: These findings indicate the benefit of PILP applications in the functional repair of dentin caries and illustrate the challenge to integrate the PILP-method into a restorative approach in minimally invasive dental procedures.

Keywords

Dental materials; dentin caries; polymer induced liquid precursor; Remineralization; collagen

1. Introduction

Numerous dental restorative materials and procedures have been developed with the aim to remineralize dentin lesions [1]. The claims however do little to address the functionality of the tissue after treatment as examination mostly relies on mineral recovery and not on tests for improved mechanical properties. Functional mineralization is attained when there is sufficient apatite formation to reinforce dentin collagen due to intrafibrillar mineralization [2,3]. The hierarchical arrangements of hydroxyapatite (HA) in the collagen matrix ranging from nanometer to macroscopic scales has led to the complex morphologies and excellent biomechanical properties of dentin. Recently PILP (Polymer-Induced Liquid Precursor) based approaches have gained momentum as a restorative to facilitate the restoration of mechanical properties of the tissue which is critical for regaining its function. To date, the PILP-methodologies seems to be the most suitable approach to reintroduce mineral into collagen fibrils and restore tissue properties, either partially or fully [4–6]. The present study is a continuation of our long-term goal of translating the PILP treatments [4–6] into clinically viable treatments.

Thus, the aims of this paper are as follows. First, to show if PILP-solution treatments can functionally remineralize deep artificial dentin lesions (approximately 700 μm depth of demineralized zone) just like shallow lesions (150 μm demineralized zone) as shown previously [3,6–8]. Second, to design a conditioner based on pAsp and test if the conditioner-solution can remineralize PILP. Third, we developed a novel cement that is comprised of pAsp, by reaction with bioglass (BG). We are testing if the PILP-conditioner treatments can be improved with the PILP-cement application when utilized prior to final

restoration in natural lesions as well as artificial lesions. In addition to 150 μm lesion size, the 700 μm artificial dentin lesions were employed as they have reached the size of clinical significance. In the remineralization solutions, the precipitation of calcium-phosphate tends to occur at the surface of the lesions, and if lesions are shallow it becomes difficult to discern if lesions remineralize from the bottom up by diffusion of PILP-nanodroplet into the demineralized zone. Using lesion of 700 μm depth permits determination of the origin of the remineralization process and defines zones for analysis of tissue repair [9].

The ability of the PILP-method for mineralization of fibrillar collagen has been well established by our group [4–6] and others [3,7,10–12]. The PILP-method relies on the ability of highly charged macromolecules (e.g. pAsp, osteopontin, phosvitin among others) to stabilize calcium phosphate ions in the form of hydrated nanodroplets, hence, preventing homogeneous crystal nucleation and precipitation. The mechanism of the PILP-process on biomimetic regulation of collagen mineralization in the intrafibrillar lumen has been addressed in the literature [6,8,13]. Bioactive glass is known for its excellent ability to form apatite in bone regeneration in vivo [14]. Recent studies have suggested bioactive Bioglass^{R} to be used for remineralization of the dentin when integrated into restorative materials as a filler [10,15,16]. Herein, we synthesized novel cement formulations based on commercial Bioglass^{R} as a filler, which we hypothesized could set through interactions with pAsp through the glass ionomer reaction. It is presumed that hydrolyzed bioglass releases ions of calcium (Ca^{2+}) which will form ion bridges between the 200-mer long pAsp macromolecules resulting in solidification as a cement.

To date, most published research has utilized sectioned dentin slabs of the resin–dentin interface or artificially created carious lesions, most of which have shallow zones of less than 150 μm of demineralized depth. These slabs are immersed in a metastable remineralization solution containing supersaturated calcium and phosphate ions, as well as the biomimetic process directing agent capable of generating PILP nanodroplets. It has been shown that poly(anionic acid)-stabilized nanodroplets can readily diffuse into the collagen network within a sectioned slab in ways that are simply not applicable clinically [9,10]. To provide more clinically pertinent data about the remineralization competency of dental materials, we first applied the novel PILP-releasing restoratives into shallow lesions with 150 μm depth and then deep artificial lesions (approximately 700 μm depth of demineralized zone) and measured changes of the elastic modulus and hardness via nanoindentation before and after treatment. In addition, we initiated a pilot study on the natural lesions monitoring the lesion recovery by microcomputed tomography (μCT) [1]. μCT is a non-destructive research technique to study mineral density volumetrically in hard tissue such as dentin and enamel. Due to its sensitivity to changes in mineral concentration with time and position, it allows for the non-invasive collection of detailed quantitative data of a substrate before and after a specific treatment. Herein, this technique applied to natural lesions to study mineral recovery by longitudinal tracking of changes in mineral densities into the depth of a lesion that can be precisely measured through calibration with HAP phantoms and comparison of the attenuation in x-ray intensities relative to the surrounding sound dentin [17,18].

2. Materials and Methods

2.1 Artificial Lesion Preparation

Human third molars were extracted as part of a clinical treatment plan and obtained from the UCSF dental hard tissue specimen core according to protocols approved by the UCSF Committee on Human Research. After extraction, the teeth were sterilized with gamma radiation and stored intact in de-ionized water at 4 °C [19]. Sound teeth were selected and preparation of shallow and deep artificial dentin blocks (3-4 mm thick) was followed according to previously published procedures [20]. Briefly, dentin blocks measuring 3–4 mm in thickness were cut from the mid-coronal section of the teeth perpendicular to the tubule direction. A 9.5 mm core drill was applied to remove the circumferential enamel and to achieve a uniform specimen of dentin. The occlusal surfaces were ground with SiC abrasive papers from 320 to 1200 grit and then polished with aqueous diamond suspensions (Buehler, Lake Bluff, IL) of 6.0, 3.0, 1.0, and 0.25 μm particle sizes. Each sample surface was covered in nail varnish (Revlon Nail Enamel #270, New York, NY) excluding a window approximately 2.5 x 2.5 mm prior to soaking in demineralizing solution consisting of 0.05 M acetate buffer, 2.2 mM calcium and phosphate at pH 4.5 for 168 hours to create deep lesions (~700 μm) and at pH 5 for 66 hours to create shallow lesions (~150 μm) on a 3-D rotating plate at 37 °C [21]. Samples then were thoroughly washed, the bottom side etched using 37% phosphoric acid gel, and nail varnish removed except for a small area that was used as a reference of sound dentin for analysis. Samples then were separated into treatment groups (n=3) replicating the treatments of the natural lesions (n=3) (Table 1) and undergoing remineralization for two and four weeks for shallow and deep lesions, respectively, at 37 °C while being continually rocked for a period of treatment. Cement and conditioner, and the PILP solution were prepared as described below. Finally, restored samples were soaked in simulated body fluid (SBF) solution, prepared as previously described [21]. After remineralization, samples were sectioned through the center of the lesion and polished as described elsewhere [21].

PILP Solution (n=3 for deep lesions): A group consisting of PILP-remineralizing solution was tested. Buffer containing Tris, 4.5 mM calcium, 2.1 mM phosphate at pH 7.4, and 0.1 mg/ml of pASP (27kD Alamanda-Polymer, USA) was added to the study. For the sample in the PILP-solution group after demineralization samples were dropped into 40 mL of PILP-solution which was replaced at two weeks.

PILP conditioner (n=3 for shallow and n=3 for deep lesions): The conditioner (con) was prepared in remineralizing buffer containing Tris-HCl, 4.5 mM calcium and 2.1 mM phosphate at pH 7.4, and 5 mg/ml of 27kD poly-L-aspartic acid (pASP) sodium salt, as described previously [20]. The demineralized samples for this group were dried gently with compressed air for 15 s. Then, 20 μl of conditioner was applied to the dentin surface through the 2.5 x 2.5 mm^2 window of demineralized specimens for 20 s. The restorative material of RMGIC (BC) was placed onto the lesion surface and light-cured for 30 s before immersion into SBF solution. This group is called con-BC.

PILP-cement (n=3 for shallow and n=3 for deep lesions): Commercial Bioglass also known as 45S5 was developed by Hench [22] and used for this study to create a dental cement. A

mixture of pAsp (27Kd, Alamanda, Huntsville, AL) and pAsp (23Kd, Alamanda, Huntsville, AL) was used in the cement composition to achieve appropriate cement setting times. The ratio of pAsp mixture was adjusted following pAsp (27kd): pAsp (23kd): 80:20 by weight. A PILP-releasing cement (lin) was made by mixing bioglass powder: pAsp: H_2O at the ratio of 40 (mg): 20 (mg): 22 (μl) respectively, where the pAsp mixture was dissolved in H_2O first. Subsequently, all the components of the cement were mixed thoroughly until homogenous using a plastic spatula. The cement was left for 2 minutes to complete initial setting times prior to the application onto the lesion. The resultant cement was non-radiopaque. The demineralized samples for this group were dried gently with compressed air for 15 s. Then, 20 μl of conditioner was applied for 20 s to the 2.5 × 2.5 mm^2 window of the demineralized zone. Next, PILP-conditioner (con) was applied as described above, before the cement liner was applied to a moist surface of demineralized zone using a spatula. Last, restorative material of RMGIC (BC) was placed onto the lesion surface after 2 min of the application of cement on the surface and light-cured for 30 s before proceeding to the SBF soaking. This group is called con-lin-BC.

RMGIC (BC) (n=3 for shallow and n=3 for deep lesions): For the control group specimens were restored without PILP-treatment using the resin-modified glass-ionomer Biocem (Nusmile, Houston, TX, USA). The demineralized samples for this group were dried gently with compressed air for 15 s. Then the specimens were rehydrated with 20 μl of de-ionized water and kept moist before the application of RMGIC emulating the PILP-conditioner treatment.

2.2 Artificial lesions characterization

Nanoindentation—After the remineralization period was finished, specimens were removed from SBF, gently rinsed with de-ionized water, and air-dried. The blocks containing the lesions were embedded in room-temperature curing epoxy (Epoxicure, Buehler, Ltd., Lake Bluff, IL). Then each specimen was sectioned through the 2.5 × 2.5 mm^2 window. The cross-section was ground with abrasive papers from 320 to 1200 grit, and then polished with aqueous diamond suspensions (Buehler, Lake Bluff, IL) of 1.0, and 0.25 μm particle size. The sectioned and polished dentin blocks were then fixed in a wet cell, and hydrated with deionized water to prepare for nanoindentation as previously described elsewhere [20]. Subsequently, all groups (n=3) were studied with a transducer-based nanoindenter (Hysitron Inc., Minneapolis, MN) attached to an atomic force microscope (MultiMode, Nanoscope IIIa Controller, Bruker-Nano Inc.) using a Berkovich diamond testing probe as previously described [4,5,23,24]. Two rows of indents spaced 20 μm were taken moving sagittally from the lesion-cement interface to sound dentin for both shallow (150 μm) and deep lesions (700 μm). For shallow lesions, two lines of nanoindents were placed for each sample and three samples per group analyzed (n=3). For deep lesions, four lines of nanoindents were placed for each sample and three samples per group analyzed (n=3). Average modulus and hardness data were graphed for each group with the first data point corresponding to the lesion surface at 0 μm. The distance was determined through measuring the distance from sound dentin adjacent to the lesion surface when fully hydrated with deionized water.

Scanning Electron Microscopy—Selected specimens were also analyzed by SEM (Quanta, FEI, Thermo Fisher Sci, USA) operating at 15 kilovolts with elemental analysis (EDS) (X-Max, Oxford Instruments, UK). Line profiles of elemental contents were recorded for C, P and Ca at a working distance at about 10–12 mm Samples were sputter coated with Pd-Au about 80 nm thickness prior to analysis.

pAsp-release kinetics—The release of pAsp from the deep artificial lesions was measured using CBQCA protein quantification kit (ThermoFisher Scientific, Waltham, MA) according to manufacturer instruction. The kit utilizes the ATTO-TAGCBQCA reagent (3-(4-carboxybenzoyl)quinoline-2-carboxaldehyde), a highly sensitive chromatographic derivatization reagent, it reacts with primary amines in the presence of cyanide. The artificial lesions were treated and then soaked in SBF. Aliquots of SBF from each treatment group we removed at different timepoints and the supernatant was measured for the release of pAsp. Following the steps from manufacturer, the final fluorescence signal was measured at emission at 550 nm with excitation at 465 nm in a microplate reader. A standard curve was created using different dilution series of poly aspartic acid in SBF, and then corresponding concentration of the samples was determined from the standard curve.

2.3 Natural Lesions

Selection of natural dentin lesions—Teeth included in this portion of the study underwent the same extraction procedures and sterilization as the samples used for the artificial lesion study. From the bulk of extracted molars, those presenting occlusal carious lesions were selected, and a radiograph was taken to identify the dentin lesions. From the radiographic images, teeth without dentin-caries or those with pulpal exposure were excluded from this study. Teeth with moderate lesions when at least the inner third of dentin lesion still present were selected for this study (Figure 1). All the lesions selection was supervised by a dentist with 35 years' experience in dental restorations. Before caries excavation, each tooth was scanned using μCT following the acquisition settings described at *2.4.* the root was cut from each tooth before μCT scan. The μCT projections obtained for both the baseline and treated caries stacks were reconstructed with Aviso lite 9.5 (Fisher Scientific, Hampton, NH, USA) based on a built-in algorithm.

Minimal invasive preparation of natural caries lesion—The selected teeth were then prepared using commercially available high speed and low speed electric headpiece followed by a water rinse according to minimal invasive dentistry (MID) practices [17,25]. All enamel overhangs from each carious lesion were carefully removed with a high-speed electric hand piece under water cooling until the underlying dentin lesion was exposed. The infected portion of the dentin lesion was excavated with large round bur using slow speed dry (no water spray). Procedure was terminated when the affected area of dentin was reached. The caries-removal endpoint was achieved when a hard cavity floor was felt consistently upon gentle pressure with a blunt dental explorer [17] (Figure 1).

Mineralization of natural caries lesions—After preparation following MID, teeth were treated in groups as shown in Table 1. The treated teeth with PILP (i.e con, or con-lin) as well as control (no PILP treatment) specimens were restored with non-fluoride releasing

glass ionomer, BioCem (BC) (NuSmile, Houston, TX, USA) (RMGIC), the same control used for artificial lesions (Figure 1). The conditioner was applied to the floor of the cavity with dental brush prior to application of RMGIC (BC) or liner cement (lin). Our liner was applied aiming for a thickness of up to 0.5 mm on the floor of the cavity preparation prior to final restoration by an expert dentist. Finally, the treated samples were soaked in SBF solution [20], which was replaced every month.

2.4 Microcomputed tomography

To determine the mineral density (MD) and volume percentage of the lesion, scanning was performed with a spatial resolution of 10 μm. Projection images were collected at 90 kV and 200 IA using 360° rotations, with 500 ms exposure time. Signal-to-noise ratio was improved by averaging of 30 frames during the reconstruction phase using the NRecon software (V6.5-3). After image reconstruction, two dimensional (2-D) slices in the sagittal plane were obtained using data viewer and saved in a 256-grayscale format. The same parameters were used throughout the course of this study. Virtual serial, sagittal sections derived from each tooth were used to create a 2-D stacked image using Aviso. The grayscale attenuation values were then calibrated to density by aviso software using calibration curve derived from five HA phantoms made of calcium hydroxyapatite powder embedded in epoxy resin, at five different mineral densities (19.83, 95.53, 201.54, 400.19, and 768.52 mgHA/cm^3) (Skyscan, Brucker micro CT, UK).

Thereafter, the stacked 2-D images were imported into Aviso to align the orientation of 2-D slices at the different time points (1d, 1mo, 3mo) and to implement calibration using the MD standard curve obtained by HA phantoms. The effectiveness of the treatments was evaluated by means of two parameters: (1) mineral density (MD) throughout sectional analysis at the ROI, and (2) average volume of the lesion associated with certain MDs.

2-D Mineral density: The aligned 2-D slices were then imported to image J (NIH, Bethesda, MD, USA) to determine an overall mineral line profile within a standardized region of interest (ROI). The ROI include a vertical line extending from approximately one third of enamel to the end of the carious lesion depth where MD at the cavity was still below the dentin-caries cut-off point (1.11 g/cm^3 HA)[17]. For each section (three sections per specimen), three ROIs at three different locations of lesion, including the central and the lateral portions of the lesion were analyzed as the mineral density can vary vertically and longitudinally. The length scale of the ordinate in the overall mineral profile was expressed in millimeters and as a function of lesion depth. The obtained mineral profile was then transported and plotted via Origin Pro version 9 (OriginLab, Northampton, MA) to calculate mineral recovery as function of area under peaks for the described ROI (e.g., blue highlighted rectangle, Figure 5). The difference between the integrated densities for the lesion as calculated by area under curve at ROI was subtracted from the baseline to acquire the integrated recovery of mineral density [10,26,27]. The measurement was replicated in 3 teeth and 3 virtual sagittal slices per teeth, within three ROIs within each slice (n=27 measurements) to measure final mineralization efficacy. Remineralization efficacy was calculated using $((A_1 – A_{n\ weeks})/A_1 * 100\%)$, where A_1 is the initial measurement at the

first time point and where $A_{n\ weeks}$ shows the mineral density in the lesion at various time point [18].

Caries volume change: In addition to MD, the change of caries volume over time was evaluated using Aviso lite 9.5 to be complementary to our 2-D analysis. If the MD was higher than the cut-off point (1 g/cm^3 HA), the dentin was considered sound dentin for 3-D analysis for both baseline and any treatment intervals [3,17]. The volume segmentation was carried out using Aviso software to see the effect of PILP at distinct density zones within the range of 200-1000 mgHA/cm^3 and total volume recovery. The residual volume of caries (RC) was expressed in percentage based on this formula: ((FC-IC)/IC) * 100. The final volume of carious tissue segmented in the treated stack (FC), subtracted from the volume of the initial carious tissue (IC) divided by IC. This normalization procedure was needed to adjust for the fact that larger lesions are having larger areas of residual caries, which may affect efficiency [18, 28].

2.5 Statistics

Analysis of Covariance (ANCOVA) was performed with α of 0.05 to detect the significant effects of the treatments, where the initial lesion sizes and mineral densities before restoration considered as controlling covariates. The analysis was implemented by SPSS Statistics 22 (IL, USA). For artificial lesions, one way ANOVA followed by Tukey test was performed using α of 0.05 [32]. The minimum sample size for natural lesions is calculated using the analysis of variance ANOVA to make pairwise comparisons between the mean of the groups and 2-sided equality at a time, with α of 0.05 and desired power of .80, and standard deviation (σ) < 7% of mineral density. The n=3 of minimum sample size was obtained for our preliminary studies.

3. Results

3.1 Artificial lesions

Nanoindentations in shallow lesion (Figure 2 A) were implemented across the demineralized and remineralized lesions to compare the nanomechanical properties of the demineralized tissue to restored specimens BC, con (PILP)-BC, con-lin-BC, after remineralization treatments of 2 weeks. Each data point in the line profiles is an average E-modulus value obtained from 2-4 indentations performed at the determined distance from the dentin surface in three different samples (n= 3). As shown in the Figure 2 A, there is very soft outer zone to about 60 μm depth from the surface of the lesion toward sound dentin in the demineralized zones for the specimens of demin, which is associated with a fully mineral depleted collagen matrix. This zone shifts to the left shrinking the depth of demineralized zone from 60 μm to 40 μm for the specimens of con-BC, and BC. Nanomechanical properties gradually improved between 80 μm and 140 μm depth, where values of sound dentin (E=18.1 GPa) were obtained. Notably, an exceptional improvement was observed for the group treated with PILP cement (con-lin-BC) in the softest zone ($P<0.05$) as well as middle zone. Values of up to 15 GPa, were reached at the very outer zones and modulus achieved to a normal dentin values within about 80 μm lesion depth and remained at elevated levels all the way to the bottom of the lesion. This is a notable recovery of properties for a short period of

two weeks of remineralization. The SEM (Figure 2, B, C) produced a more noticeable gap between the cement and demineralized dentin in the sample restored with BC only (control) as well as con-BC. On the other hand, the PILP cement treatment (con-lin-BC) showed full recovery in the remineralized zone throughout the lesions regaining its structural properties like sound dentin (Figure 2, D). Using EDS-analysis, line profiles and elemental maps across the cement-dentin interface were created for BC, con-lin-BC (Figures. 3 A–D). The group of BC (control) showed a gradual depletion of calcium and phosphorous from the bottom of the lesion towards the cement interface, indicating that the remineralization process has not been fully completed in these specimens. On the other hand, con-lin-BC appears to have recovered in mineralizing ions of calcium and phosphorous showing a sudden increase in calcium and phosphorous content starting from the bottom of the lesion toward cement interface.

A similar trend in mineral profile changes was observed in deep lesions (Figure 4 A–D). Line profiles of the average elastic modulus and hardness (n=3) are graphed from lesion surface at 0 μm through the lesion to sound dentin at about 700 μm. When compared to the line profile for the demineralized specimen before treatment, all groups show a reduced lesion depth as the onset of the sloped zone moves to the left. Specimens treated with liner (con-lin-BC) showed the higher recovery in slope zone ranges from 350-700 μm. The restorative treatments did not restore much of the mechanical properties in the most demineralized regions, the very outer zones. At lesion depth of up to 300 μm, none of the treatments showed significant improvement. On the contrary, specimens treated with PILP-solution (0.1 mg/ml) performed exceptionally well and restored most of the outer lesion between 30 and 50% of sound dentin values. That significant improvement of properties is well illustrated in the average E-modulus and hardness graph (Figure. 4 C and D) for the outermost 450 μm of lesion depth, showing that lesions treated with PILP-solution reach on average 6.3 and 0.26 GPa in E-modulus and hardness, respectively. We note here, this is the first attempt to show the efficacy of the PILP-solution treatments on deep lesions (700 μm) which demonstrates that functional remineralization of dentin is initiated from the bottom of the lesion, which was not completely clear from studies on shallow lesions. With regards to samples included a restorative procedure, the group con-lin-BC had significantly increased mechanical recovery when compared to the demineralized control ($P<0.05$). Nonetheless, the BC group and con-BC group had only minimal recovery.

PILP release capability—The PILP-releasing capability was studied by measuring the pAsp concentration using fluorescence based total protein assay. The release of poly aspartic acid from artificial lesions treated with con-lin-BC, and BC was measured from day 14 to day 28 (Figure 5). The QBCA has been used in sensitive assays for detecting of Glu, Gly, Tau and GABA in rat spinal cord tissue [28]. The study on pAsp-release on artificial lesions treated with cement showed that the amount of PILP-release increased from 50 μg at day 14 to 115 μg at day 28. There is a significant difference ($P<0.05$) between control (BC) with con-lin-BC treated lesion at day 1 and 28.

3.2. Natural Lesions

Mineral recovery as function of area under peaks (AUP)—The change in MD over period of 3 months is shown in Figure 6 for natural caries treated with PILP cement and PILP conditioner and recapped with BC. The μCT images are shown on the right side and their prospective mineral density graph are shown on the left. After the remineralization period, it was observed that all three restorative treatments induced mineral gain from baseline, to 1 month, and to final 3 months as shown in graph as the intensity of the peaks increase gradually (Figure 6, A, B, C). According to μCT images and mineral density all treatments that contained PILP had predominate remineralization originating at the bottom of the lesion moving towards the lesion interface. Figure 7 represent the average of perceptual recovery in MD for different treatment groups. Different increases in mineral content were detected between the three treatment groups including PILP cement, PILP conditioner, and control. The BG-pAsp (con-lin-BC) cements increased mineral recovery in dentin with mineralization doubling from 1 month to 3 months (Figures 6, 7). The mineral recovery for con-lin-BC samples ($p<0.05$) reached 27% at 3 months compared to 21% and 15% for con-BC and BC respectively.

Mineral recovery as function of residual caries volume—In addition to sectional analysis of mineral density (MD) presented in previous Figures (6, 7), the mean volume of the residual caries was also evaluated. An example of segmentation and 3-D reconstructed volume from the 2d sections (>1000 sections/specimen) of caries for each treatment group are presented in Figure 8, (A–D). In addition, the residual volume of caries was also segmented out according to different density zones of 200-500 mg HA/cm^3, 500-700 mgHA/cm^3 and 700-1000 mgHA/cm^3 to visualize the changes that occur at each density zone as shown in Figure 8 (D) (N=1), and mean value (n=3) of total caries volume reduction shown in Figure 9. As can be seen in Figure 8 (A–D), the volume of the lowest density zones of 200-500 mgHA/cm^3 for all the examples (con-lin-BC, con-BC, and BC) decreased over 3 months. For instance, the volume of the 200-500 zones of con-BC (Figure 8 (B, purple area, at 1d) is reduced by 62% (Figure 8 D). It appears that volume of 200-500 zones at 1 day has been transformed either to 700-1000 as it replaced by pink area (Figure 8B, Pink area, at 3 mo) or sound dentin (above 1000 mgHA/cm^3, gray area in the recreated lesion). The same trend was observed for other samples of the con-lin-BC, and BC. Similarly, as it is shown for con-lin-BC (Figure 8C, at 1d and 3 mo), some of the area in the zones of 500-700, and 700-1000 mgHA/cm^3 were also recovered to sound dentin or in case of 500-700 mgHA/cm^3 moved to higher neighboring zones of 700-1000 mgHA/cm^3. Interestingly, the most recovery was observed in the lesion directly under enamel at the occlusal surface compared to other lesion near the proximal surface, as this particular tooth had three lesions on occlusal and proximal surfaces. As shown in Figure 9, the average volume reduction agrees with our MD results (Figures 6, 7). Different treatments led to various degrees of caries volume reduction within the overall density zone of 200-1000 mgHA/cm^3. The highest reduction occurred for the group treated with both conditioner and liner cement (con-lin-BC), where lesion volume reduced by 21% at 3 months ($P<0.05$) compared to control where it reached approximately 6% and the conditioner treatment at 15%.

4. Discussion

Herein, the PILP-method was applied in three ways: First, as a conditioner with concentrated PILP-solution (5 mg/ml pAsp). Second, in form of a cement when mixed with commercial bioglass, and third in form of PILP solution with 0.1 mg/ml pAsp. Our study indicated that the collagen matrix can be functionally remineralized with our PILP treatments of deep lesions, and by a PILP-releasing cement in shallow lesion as indicated by improved nanomechanical properties (Figures 2, 4). The present study also demonstrated a successful PILP application in natural lesions in a clinically adaptable dental setting using a cement liner that releases pAsp. Both PILP-delivery methods lead to mineral recovery and reduce the demineralization depth over their respective controls for both the artificial as well as natural lesions (Figures 2–4, 8–9) ($P<0.05$) with regards to elastic modulus recovery and the lesion volume reduction. However, achieving full recovery across both deep artificial lesions and natural lesions was not feasible with the current PILP-restorative treatments, while immersion into PILP solution proved to repair deep lesions to a much greater and significant extend [1,3,8,12].

The most significant improvement in elastic modulus and hardness over RMGIC control was observed for con-lin-BC in the shallow lesion ($P<0.01$) as well as PILP solution in deep lesions (700 μm demineralized zone) ($P<0.05$) compared to RMGIC, and at the middle zone on the deep lesions as the residual mineral reinforced the collagen fibrils at increasing levels between 80 μm and 140 μm depth compared to demin control ($P<0.05$). We hypothesize that pAsp would infiltrate into the collagenous matrix of demineralized dentin in the form of PILP-nanodroplets and initiate the biomineralization process by release of calcium and phosphate ions into the lumen of the collagen fibrils, as can be confirmed by EDX and SEM analysis as well as PILP release study on Figure 3 A–D, and Figure 5, respectively. On the other hand, the EDX and SEM analysis shows a more noticeable gap in the samples treated with BC, or con BC (Figure 3) which is due to dentin substrate further contracting because of dehydration in the vacuum thereby indicating that the lesion has not been fully functionally remineralized, resulting in delamination of the cement from the dentin substrate surface. Delamination did not occur with con-lin-BC.

The obtained data on release of pAsp (Figure 5) suggested that pAsp was released at the dentincement interface which initiated the PILP-mineralization process by interaction with SBF diffusing through the dentin tubules. Thus, the pAsp-bioglass cement, capable of enhancing the remineralizing dentin lesions, represents a novel and promising PILP-approach in caries management [29].

Moreover, this study demonstrated the implementation of the PILP approach into natural lesions in human molars evaluated by μCT for mineral density and volume changes in the lesions. The majority of studies on remineralization of dentin are based on growth of calcium phosphate phases over remnant seed crystallites, in compliance with the principles of the classical theory of crystallization [30–32]. Nonetheless, our volumetric analysis of μCT data shows recovery of mineral content in carious zones at densities of 200-500 mgHA/cm^3 (Figure 8) which are most likely devoid of seed HA crystallites but capable to form mineral de novo. We hypothesized that the higher volume recovery on con-lin-BC

($P<0.05$) (Figure 9) can be attributed to the sustained supply of Ca^{2+} and PO_4 ions forming ion clusters [29,33] from a gradual dissolution of the cement. In general, natural lesions are more difficult to remineralize due to their variability in lesion depths and degrees of tubular occlusion [30]. Another limitation of our study is, that unlike artificial caries, demineralization in real human caries-affected dentin is often displayed as irregular islands of demineralization instead of a continuous demineralization gradient from the lesion surface to the lesion base [31,33]. Overall, we believe that PILP formulations can improve functional remineralization according to our preliminary results. However, synthesis of formulations of cement compositions that provide substantial amounts of mineral ions and process-directing molecules for release into collagen matrices appear favorable to improving the depth of mineralization and potential full recovery in both deep artificial and natural lesions [34].

5. Conclusion

This initial study presented supporting data that integration of the PILP-process in a restorative dental treatment such as a liner cement or as a conditioner is feasible and promotes functional remineralization of demineralized dentin in artificial deep lesions. Moreover, our pilot study on natural lesions warrant a continuous investigation of the PILP-based approach for the functional repair of caries as part of minimally invasive dental procedures. Nonetheless, there is still much work to be done on translating the PILP-method into the dental clinic and to fully unfold the potential of process-directing agents of biomineralization in repairing caries-affected dentin.

Acknowledgments

This work was supported by NIH/NIDCR RO1 DE016849, R21 DE028421 and by UCSF Catalyst Award “PILP Treatment for the Repair of Dental Caries” and by the Center for Dental, Oral and Craniofacial Tissue & Organ Regeneration” (C-DOCTOR-NIH/NIDCR U24DE026914), as well as NSF I-Corps 2033171. Micro-CT imaging support was provided through the Core Center for Musculoskeletal Biology and Medicine (CCMBM) at UCSF through NIH-grant P30-AR066262.

References

[1]. Fernando D, Attik N, Pradelle-Plasse N, Jackson P, Grosgogeat B, Colon P, Bioactive glass for dentin remineralization: A systematic review, Materials Science and Engineering: C. 76 (2017) 1369–1377. 10.1016/j.msec.2017.03.083. [PubMed: 28482504]

[2]. Taha AA, Patel MP, Hill RG, Fleming PS, The effect of bioactive glasses on enamel remineralization: A systematic review, Journal of Dentistry. 67 (2017) 9–17. 10.1016/j.jdent.2017.09.007. [PubMed: 28939485]

[3]. Qi Y, Li N, Niu L, Primus CM, Ling J-Q, Pashley DH, Tay FR, Remineralization of artificial dentinal caries lesions by biomimetically modified mineral trioxide aggregate, Acta Biomaterialia. 8 (2012) 836–842. 10.1016/j.actbio.2011.10.033. [PubMed: 22085925]

[4]. Bertassoni LE, Habelitz S, Marshall SJ, Marshall GW, Mechanical recovery of dentin following remineralization in vitro — An indentation study, Journal of Biomechanics. 44 (2011) 176–181. 10.1016/j.jbiomech.2010.09.005. [PubMed: 20926080]

[5]. Habelitz S, Marshall GW, Balooch M, Marshall SJ, Nanoindentation and storage of teeth, Journal of Biomechanics. 35 (2002) 995–998. 10.1016/S0021-9290(02)00039-8. [PubMed: 12052404]

[6]. Saxena N, Habelitz S, Marshall GW, Gower LB, Remineralization of demineralized dentin using a dual analog system, Orthodontics & Craniofacial Research. 22 (2019) 76–81. 10.1111/ocr.12271. [PubMed: 31074152]

[7]. Sun J, Chen C, Pan H, Chen Y, Mao C, Wang W, Tang R, Gu X, Biomimetic promotion of dentin remineralization using l-glutamic acid: inspiration from biomineralization proteins, J. Mater. Chem. B 2 (2014) 4544–4553. 10.1039/C4TB00451E. [PubMed: 32261555]

[8]. Kim J, Arola DD, Gu L, Kim YK, Mai S, Liu Y, Pashley DH, Tay FR, Functional biomimetic analogs help remineralize apatite-depleted demineralized resin-infiltrated dentin via a bottom–up approach, Acta Biomaterialia. 6 (2010) 2740–2750. 10.1016/j.actbio.2009.12.052. [PubMed: 20045745]

[9]. Saeki K, Chien Y-C, Nonomura G, Chin AF, Habelitz S, Gower LB, Marshall SJ, Marshall GW, Recovery after PILP remineralization of dentin lesions created with two cariogenic acids, Archives of Oral Biology. 82 (2017) 194–202. 10.1016/j.archoralbio.2017.06.006. [PubMed: 28647649]

[10]. Niu L, Zhang W, Pashley DH, Breschi L, Mao J, Chen J, Tay FR, Biomimetic remineralization of dentin, Dental Materials. 30 (2014) 77–96. 10.1016/j.dental.2013.07.013. [PubMed: 23927881]

[11]. Zhang Y, Wang Z, Jiang T, Wang Y, Biomimetic regulation of dentine remineralization by amino acid in vitro, Dental Materials. 35 (2019) 298–309. 10.1016/j.dental.2018.11.026. [PubMed: 30545612]

[12]. Niu L, Jee SE, Jiao K, Tonggu L, Li M, Wang L, Yang Y, Bian J, Breschi L, Jang SS, Chen J Pashley DH, Tay FR, Collagen intrafibrillar mineralization as a result of the balance between osmotic equilibrium and electroneutrality, Nature Materials. 16 (2017) 370–378. 10.1038/nmat4789. [PubMed: 27820813]

[13]. Gower LB, Biomimetic model systems for investigating the amorphous precursor pathway and its role in biomineralization, Chem Rev. 108 (2008) 4551–4627. 10.1021/cr800443h. [PubMed: 19006398]

[14]. Liu X, Rahaman MN, Fu Q, Bone regeneration in strong porous bioactive glass (13-93) scaffolds with an oriented microstructure implanted in rat calvarial defects, Acta Biomaterialia. 9 (2013) 4889–4898. 10.1016/j.actbio.2012.08.029. [PubMed: 22922251]

[15]. Yoshikawa H, Myoui A, Bone tissue engineering with porous hydroxyapatite ceramics, Journal of Artificial Organs. 8 (2005) 131–136. 10.1007/s10047-005-0292-1. [PubMed: 16235028]

[16]. Zandi Karimi A, Rezabeigi E, Drew RAL, Glass ionomer cements with enhanced mechanical and remineralizing properties containing 45S5 bioglass-ceramic particles, Journal of the Mechanical Behavior of Biomedical Materials. 97 (2019) 396–405. 10.1016/j.jmbbm.2019.05.033. [PubMed: 31174045]

[17]. de A. Neves A, Coutinho E, De Munck J, Van Meerbeek B, Caries-removal effectiveness and minimal-invasiveness potential of caries-excavation techniques: A micro-CT investigation, Journal of Dentistry. 39 (2011) 154–162. 10.1016/j.jdent.2010.11.006. [PubMed: 21111770]

[18]. Delbem ACB, Sassaki KT, Vieira AEM, Rodrigues E, Bergamaschi M, Stock SR, Cannon ML, Xiao X, De Carlo F, Delbem ACB, Comparison of Methods for Evaluating Mineral Loss: Hardness versus Synchrotron Microcomputed Tomography, Caries Research. 43 (2009) 359–365. 10.1159/000231573. [PubMed: 19648747]

[19]. Brauer DS, Saeki K, Hilton JF, Marshall GW, Marshall SJ, Effect of sterilization by gamma radiation on nano-mechanical properties of teeth, Dental Materials. 24 (2008) 1137–1140. 10.1016/j.dental.2008.02.016. [PubMed: 18436298]

[20]. Bacino M, Girn V, Nurrohman H, Saeki K, Marshall SJ, Gower L, Saeed E, Stewart R, Le T, Marshall GW, Habelitz S, Integrating the PILP-mineralization process into a restorative dental treatment, Dental Materials. 35 (2019) 53–63. 10.1016/j.dental.2018.11.030. [PubMed: 30545611]

[21]. Chien Y-C, Burwell AK, Saeki K, Fernandez-Martinez A, Pugach MK, Nonomura G, Habelitz S, Ho SP, Rapozo-Hilo M, Featherstone JD, Marshall SJ, Marshall GW, Distinct decalcification process of dentin by different cariogenic organic acids: Kinetics, ultrastructure and mechanical properties, Archives of Oral Biology. 63 (2016) 93–105. 10.1016/j.archoralbio.2015.10.001. [PubMed: 26745819]

[22]. Hench LL, The story of Bioglass®, Journal of Materials Science: Materials in Medicine. 17 (2006) 967–978. 10.1007/s10856-006-0432-z. [PubMed: 17122907]

[23]. MURDOCH-KINCH CA, McLEAN ME, Minimally invasive dentistry, The Journal of the American Dental Association. 134 (2003) 87–95. 10.14219/jada.archive.2003.0021. [PubMed: 12555961]

[24]. Burwell AK, Thula-Mata T, Gower LB, Habelitz S, Kurylo M, Ho SP, Chien Y-C, Cheng J, Cheng NF, Gansky SA, Marshall SJ, Marshall GW, Functional remineralization of dentin lesions using polymer-induced liquid-precursor process, PLoS One. 7 (2012) e38852–e38852. 10.1371/journal.pone.0038852. [PubMed: 22719965]

[25]. Yamada T, Nakamura K, Iwaku M, Fusayama T, The Extent of the Odontoblast Process in Normal and Carious Human Dentin, J Dent Res. 62 (1983) 798–802. 10.1177/00220345830620070401. [PubMed: 6306079]

[26]. ten Cate JM, Damen JJM, Buijs MJ, Inhibition of Dentin Demineralization by Fluoride in vitro, Caries Research. 32 (1998) 141–147. 10.1159/000016444. [PubMed: 9544863]

[27]. Määrten A, Fratzl P, Paris O, Zaslansky P, On the mineral in collagen of human crown dentine, Biomaterials. 31 (2010) 5479–5490. 10.1016/j.biomaterials.2010.03.030. [PubMed: 20399496]

[28]. Şanlı N, Tague SE, Lunte C, Analysis of amino acid neurotransmitters from rat and mouse spinal cords by liquid chromatography with fluorescence detection, Journal of Pharmaceutical and Biomedical Analysis. 107 (2015) 217–222. 10.1016/j.jpba.2014.12.024. [PubMed: 25596498]

[29]. Weir MD, Ruan J, Zhang N, Chow LC, Zhang K, Chang X, Bai Y, Xu HHK, Effect of calcium phosphate nanocomposite on in vitro remineralization of human dentin lesions, Dental Materials. 33 (2017) 1033–1044. 10.1016/j.dental.2017.06.015. [PubMed: 28734567]

[30]. Pugach MK, Strother J, Darling CL, Fried D, Gansky SA, Marshall SJ, Marshall GW, Dentin caries zones: mineral, structure, and properties, J Dent Res. 88 (2009) 71–76. 10.1177/0022034508327552. [PubMed: 19131321]

[31]. Silva NRFA, Carvalho RM, Pegoraro LF, Tay FR, Thompson VP, Evaluation of a Self-limiting Concept in Dentinal Caries Removal, J Dent Res. 85 (2006) 282–286. 10.1177/154405910608500315. [PubMed: 16498079]

[32]. Eliaz N, Metoki N, Calcium Phosphate Bioceramics: A Review of Their History, Structure, Properties, Coating Technologies and Biomedical Applications, Materials (Basel). 10 (2017) 334. 10.3390/ma10040334.

[33]. Mijan MC, Frencken JE, Schwass DR, Chaves SB, Leal SC, Microcomputed Tomography Evaluation of Dentine Mineral Concentration in Primary Molars Managed by Three Treatment Protocols, Caries Research. 52 (2018) 303–311. [PubMed: 29408818]

[34]. Braga R, About I, How far do calcium release measurements properly reflect its multiple roles in dental tissue mineralization?, Clinical Oral Investigations. 23 (2019) 501–501. [PubMed: 30612242]

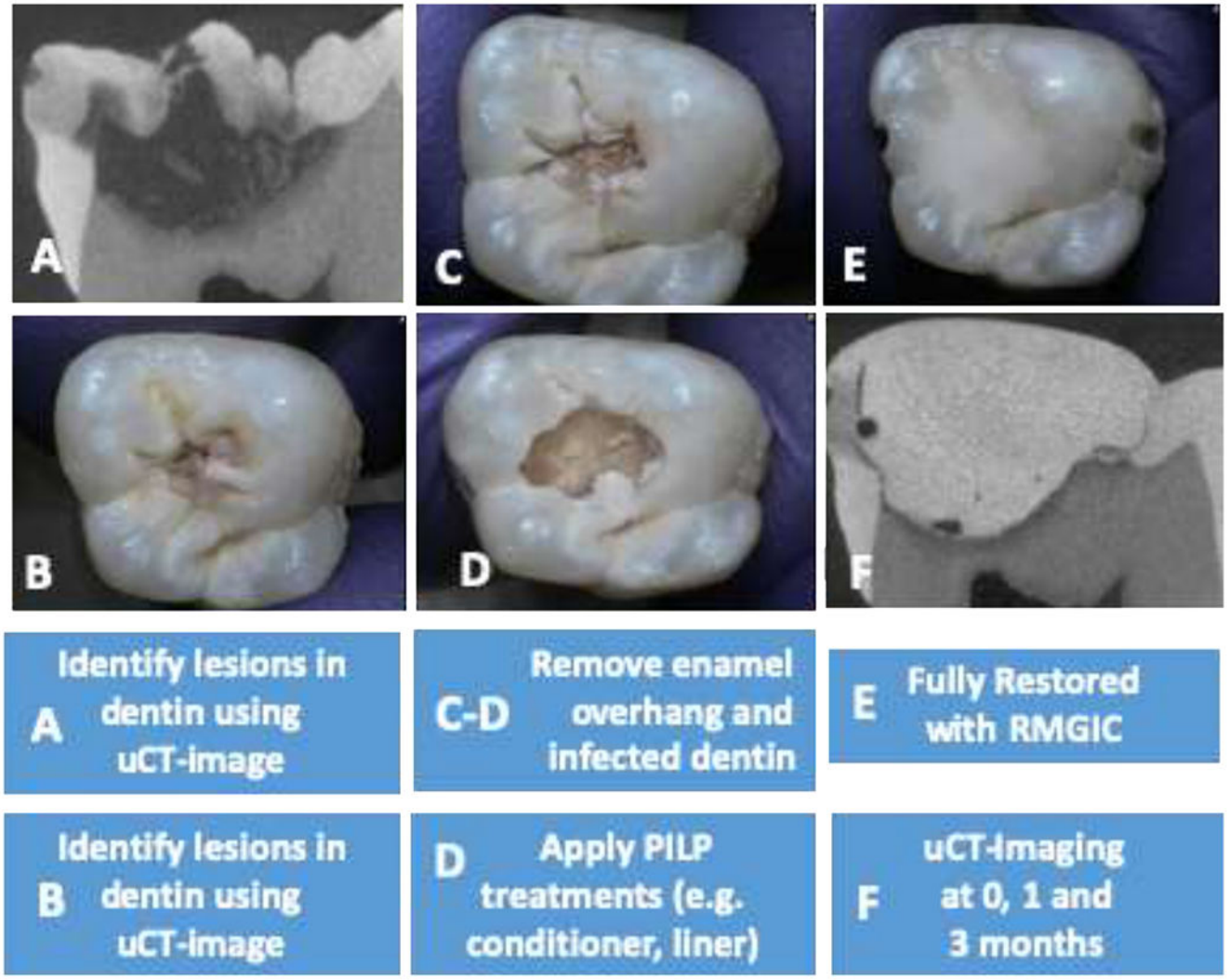

Figure 1.

Natural carious lesions minimally invasive preparation and restoration steps. (A) Human third molars presenting occlusal carious lesions were selected using dental x-ray and μCT-image. (B) Optical image of tooth before treatment. (C) Minimal removal of enamel overhang. (D) Minimal removal of affected caries dentin followed by application of PILP conditioner. (E) Cavity fully restored with RMGIC. (F) μCT-image obtained at day 1 of restoration and initiation of remineralization in SBF solution.

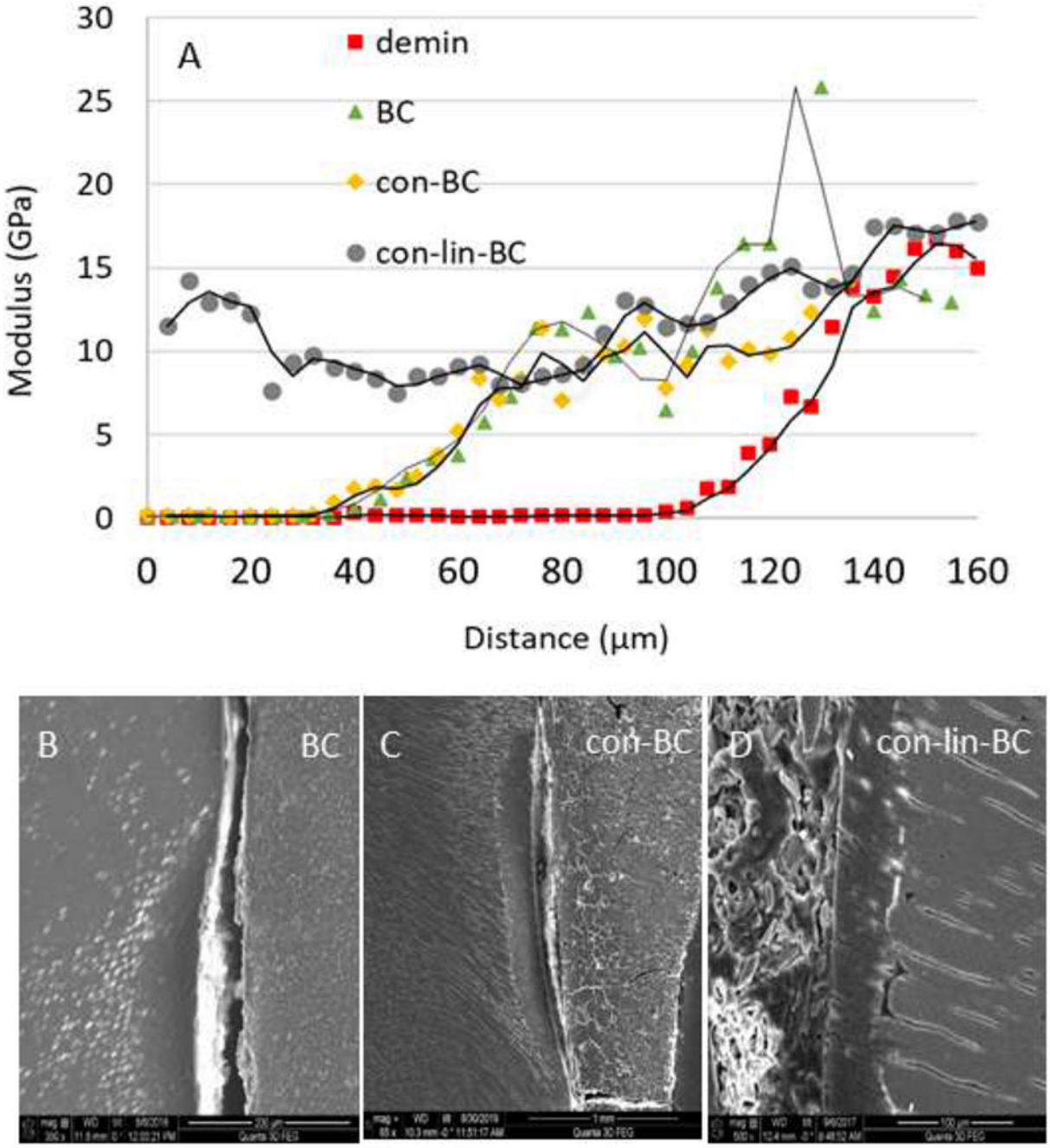

Figure 2.

(A) nano indentation study on shallow lesions. Elastic modulus values versus lesion depth obtained from nanoindentations performed along lines from the lesion surface across the lesion towards normal dentin before (demin) and after treatment. All treatments show a reduction in lesion depth as indicated by an earlier onset of the sloped region. PILP cement treatment group (con-lin-BC) showed highest significance and improvement compared to the other samples ($P<0.05$). Other groups did not show a significant improvement of the modulus in the outer zone. (B-D) SEM of specimen restored with RMGI control (no PILP)

(BC), and PILP conditioner (con-BC), and cement (con-lin-BC). Gap formation due to shrinkage was evident in the treatment groups of con-BC, and BC, whereas con-lin-BC shows full recovery.

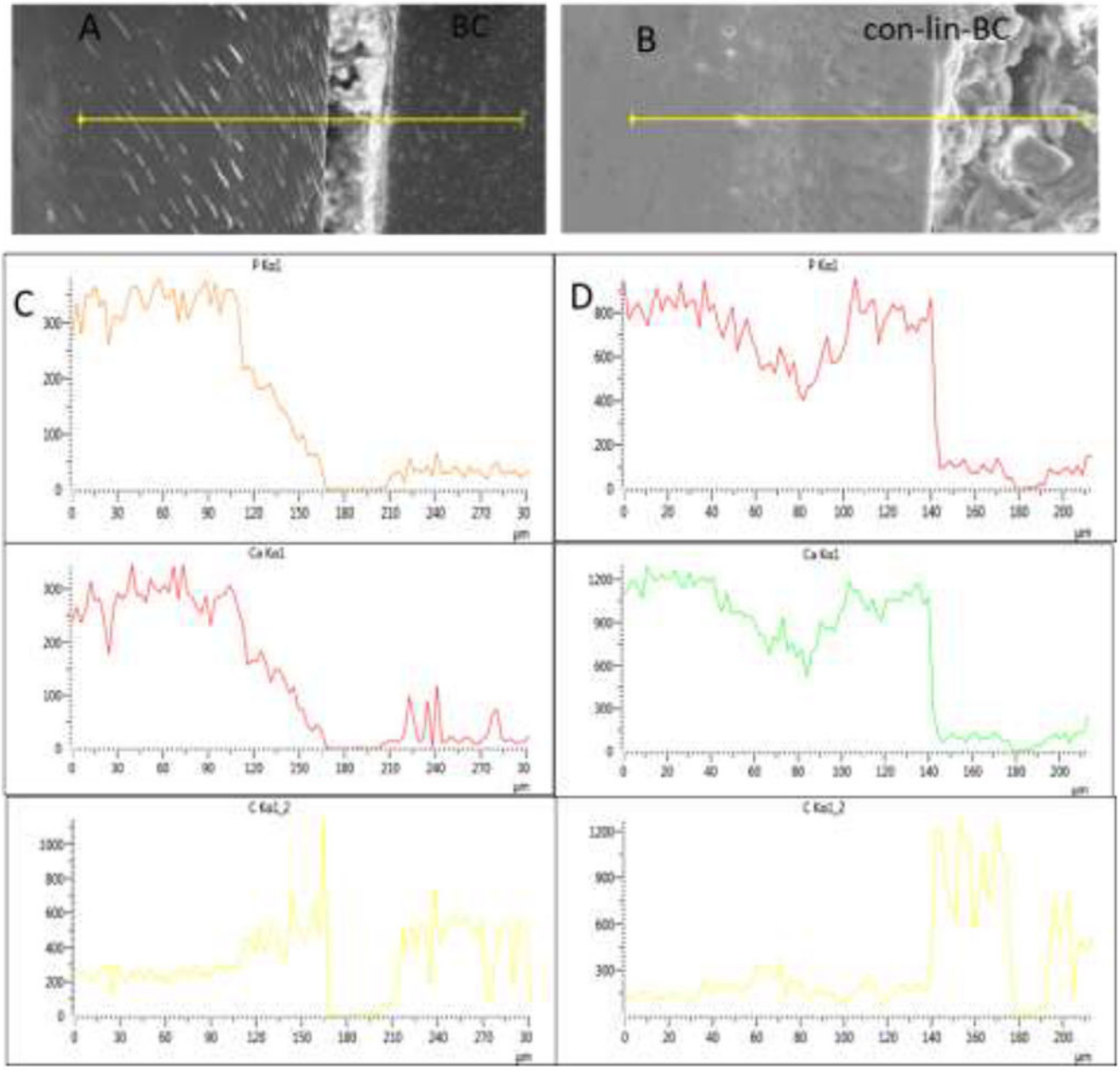

Figure 3.

(A-D) SEM-EDS-analysis by line scans on shallow lesions. Elemental concentrations (counts per sec.) of Phosphorous, Calcium, and Carbon along a line across the lesion as depicted in SEM image on top are shown for (A, C) BC, and (B, D) con-lin-BC.

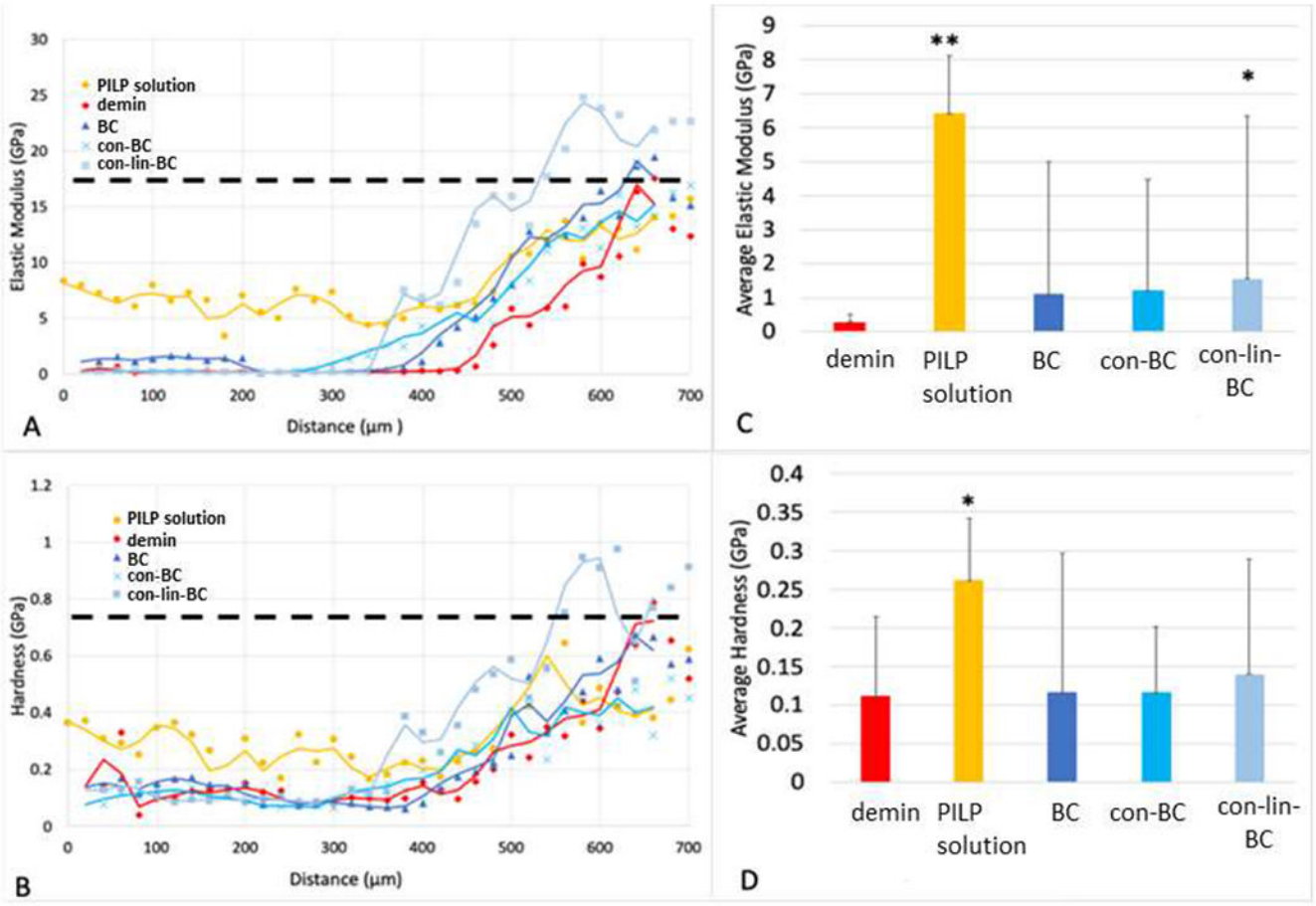

Figure 4.

Elastic modulus (A) and hardness (B) values versus lesion depth obtained from nanoindentations performed along lines from the lesion surface across the lesion towards normal dentin before (demin) and after treatment. All treatments show a reduction in lesion depth as indicated by an earlier onset of the sloped region. Average values of E-modulus (C) and hardness (D) for different treatment groups calculated from the outer portion of the lesion (first 450 µm) of corresponding line profiles. PILP-solution (0.1 mg/ml) showed highest significance and improvement compared to the demineralized samples. Only treatment group con-lin-BC showed a significantly increased E- modulus compared to demin at the slop zone. Other groups did not show a significant improvement of the modulus in the outer zone.

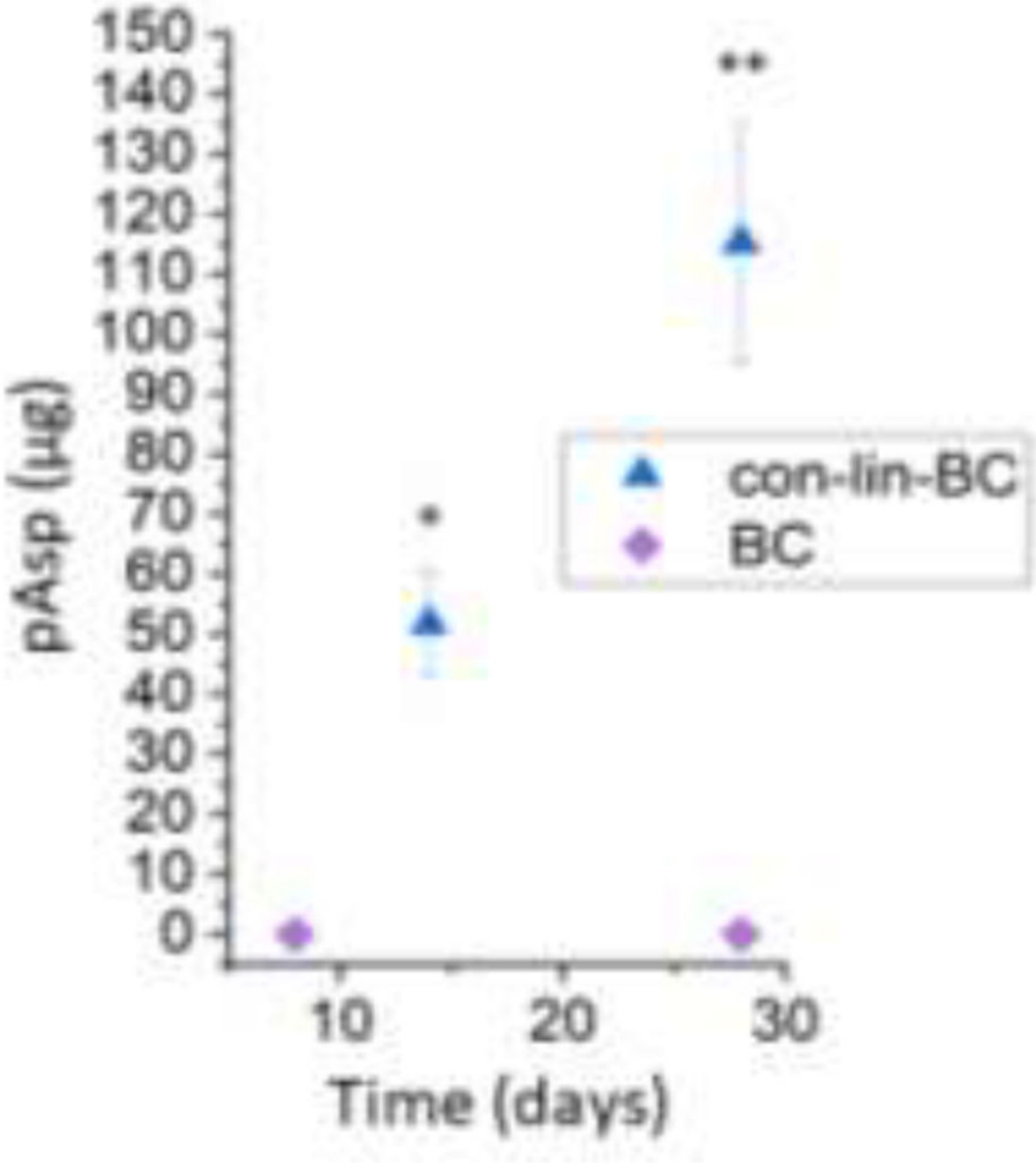

Figure 5.

PILP (Poly aspartic acid) release from artificial lesions at day 14, and 28. Artificial lesions treated with con-lin-BC showed significance PILP (Poly Asp) release at days 14, and day 28 ($P<0.05$) compared to the control artificial teeth (no PILP).

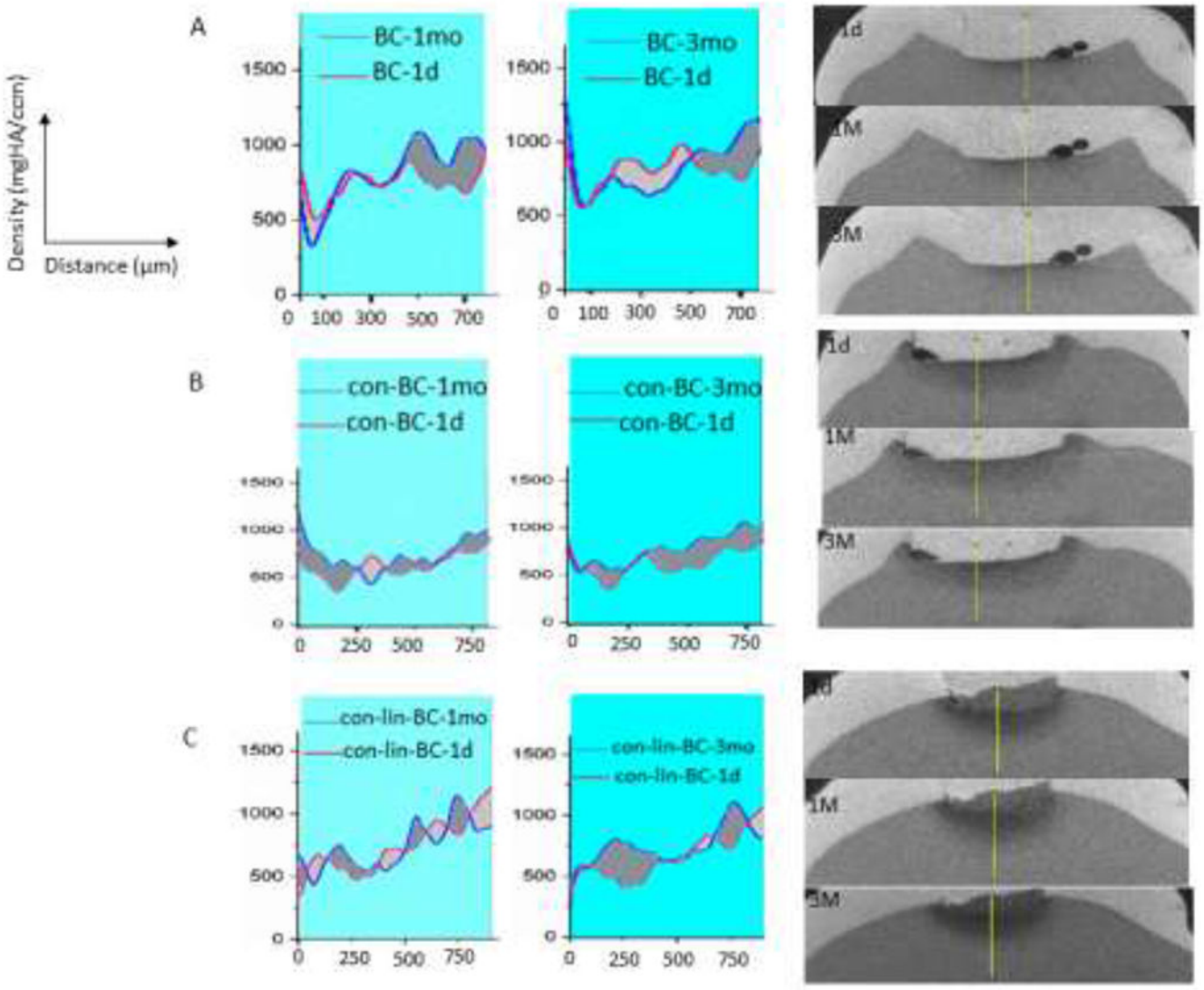

Figure 6.

On the left, Mineral density over depth of the lesions obtained from 2D scan for natural lesions treated with (A) no PILP(BC), (B) PILP conditioner (con-BC), and (C) PILP cement (con-lin-BC). Teeth treated with con-lin-BC showed highest mineral density improvement ($P<0.05$) compared to the control teeth (no PILP). On the right, corresponding μCT images of treated teeth with. (A) no PILP(BC), (B) PILP conditioner (con-BC), and (C) PILP cement (con-lin-BC) (n=3). Dark gray areas are positive and light gray areas are negative areas.

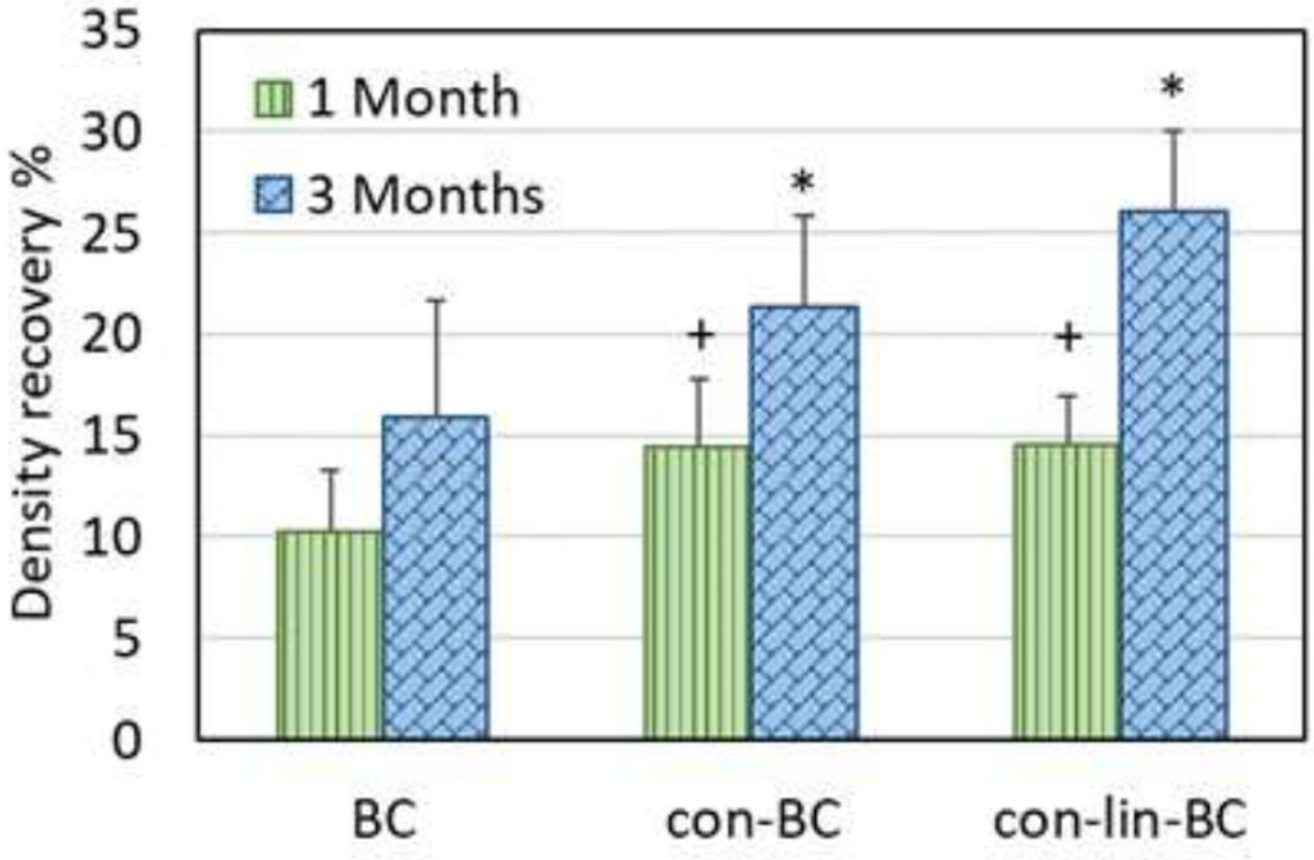

Figure 7.

Mean mineral density recovery for the lesions after 1 month and 3 months for teeth restored with PILP cement (con-lin-BC), PILP conditioner (con-BC), RMGI only (BC) at 1 and 3 months compared to 1 day. $^{*, +}$: $P<0.05$ compared to control (BC)

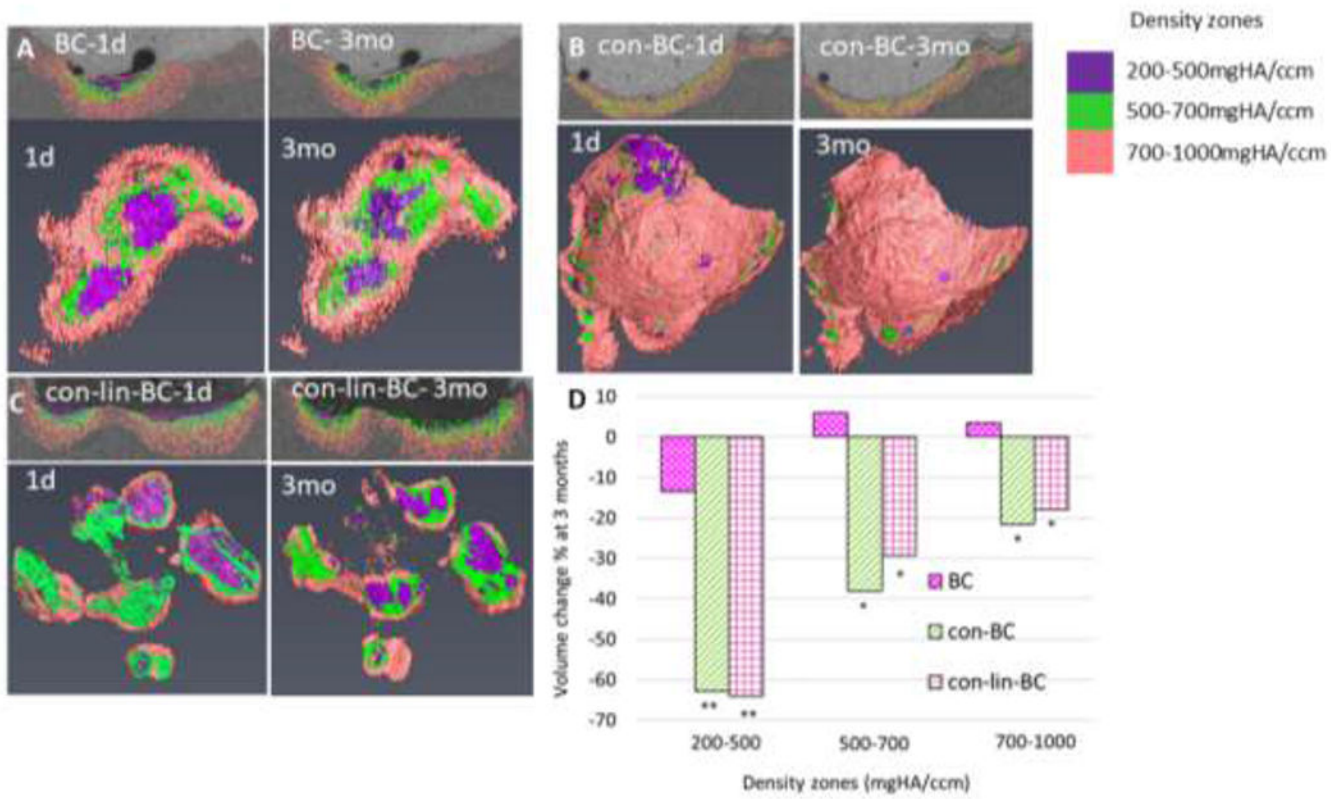

Figure 8.

Reconstructed initial caries volume and one selective 2D section (1d) and corresponding final residual caries volume, and one 2D section (3 mo) at different density zones of 200-500, 500-700, 700-1000 mgHA/cm^3 for (A) BC, (B) con-BC, (C), con-lin-BC. (D) Volume recovery percentage at each density zone 200-500, 500-700, 700-1000 mgHA/cm^3 for different treatment groups of BC, con-BC, con-lin-BC.

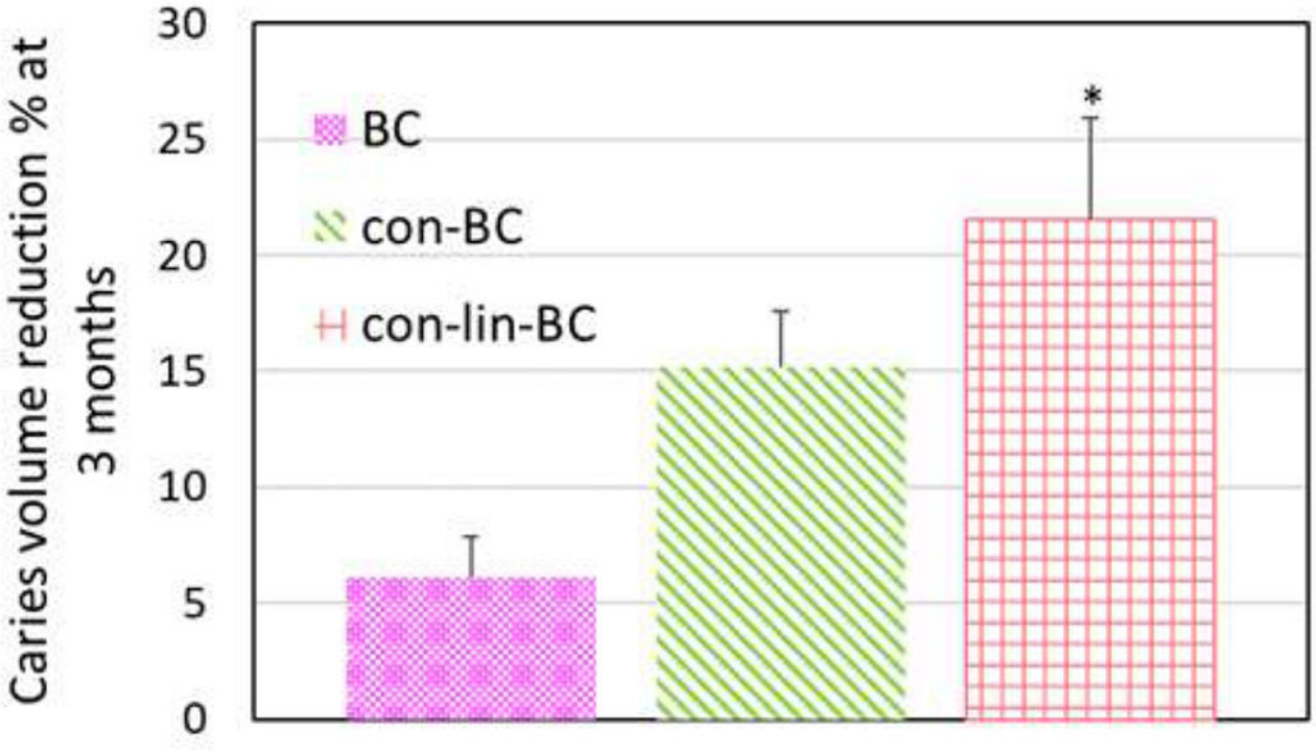

Figure 9.

Mean caries volume recovery for all treatment groups of BC, con-BC, con-lin-BC at 3 months compared to day 1 of restoration. Teeth treated with con-lin-BC showed highest volume recovery and improvement compared to the control teeth (no PILP) ($p<0.05$)

Table 1.

Natural carious lesions minimally invasive prepared and restored with different treatment groups based on PILP cement, conditioner, and no PILP and restored with RMGIC

	Conditioner	Cement Liner	Restorative	Treatment duration (months)	N
BC	H_2O	none	BioCem (Nusmile, Houston, TX, USA)	3 mo	3
con-BC	5 mg/ml pAsp	none	BioCem (Nusmile, Houston, TX, USA)	3 mo	3
con-lin-BC	5 mg/ml pAsp	Bioglass: pAsp: H_2O	BioCem (Nusmile, Houston, TX, USA)	3 mo	3